Thermal behavior of dodecylpyridinium based surfactants with varied anionic constituent

Tea Mihelj*, Vlasta Tomašić

Department of Physical Chemistry, Ruđer Bošković Institute, POB 180, Zagreb, HR–10002 Croatia

* Corresponding author:
Tea Mihelj
Ruđer Bošković Institute
Bijenička c. 54, P.O.Box 180
HR-10002 Zagreb, Croatia
Tel.: +385-1-4571-211
Fax: +385-1-4680-245
E-mail address: Tea.Mihelj@irb.hr

Keywords: dodecylpyridinium, thermotropic behavior, smectic, anionic surfactant, calorimetry, liquid crystal

Abstract

Amphiphilic molecules based on pyridinium molecule attract significant attention due to their involvement in biochemical processes. Their structure with highly interactive polar head, hydrogen bonding and π-stacking capabilities enables their potentional role in biotechnological and biomedical applications.

Three novel dodecylpyridinium based catanionic compounds were synthesized. Combination of techniques was used to examine their thermal properties; differential scanning calorimetry powder X-ray diffraction and polarizing microscopy. Briefly, the absence of mesomorphic properties and the formation of zig-zag blade textures were obtained in dodecylpyridinium picrate, thermotropic mesomorphism and polymorphism in dodecylpyridinium dodecylbenzenesulfonate, and melting accompanied with degradation in combination with cholate. The anionic part of the molecule promotes behavior of novel compounds, resulting in different packing and thermal properties of catanionics in their solid state.

1. Introduction

Self-organization is an inherent feature of living systems that took part in the first evolution processes, causing transformation from non-living into living, biologically active matter. Having this property and as well as ability to interact in different way, including some host-guest mechanisms,[1] synthetic catanionic amphiphilic systems are interesting from both, fundamental and practical viewpoint. The design of new materials, especially nanomaterials based on self-organization procedure has been one of the main focus in the field of supramolecular chemistry.[2] There is a multitude of interesting structures including micelles with different sizes and shapes,[3] bilayer vesicles[4,5] and liquid-crystalline mesophases[6] that are formed during interactions of amphiphiles. Previous studies have also reported formation of ribbons,[7,8] disks,[9] and gel-like crystalline mesophases that are used to template materials in both aqueous and/or nonaqueous domains.[10] The structure of these aggregates can be tuned by tailoring the nature of the components, and consequently, the interplay between electrostatic effects, hydrogen bonding networks, surfactant molecular size, geometry *etc*. The phase behavior of surfactant provides an appropriate starting point for analyzing complex patterns; for example, the model lipid bilayers can be prepared using non-biological building blocks of surfactants, owing their ability to form liquid crystalline phases. Besides this, such systems may provide information of the elementary mechanisms and functioning of their prototypes through biomimetics.[1] Exploration of new amphiphilic building blocks is an important task since this makes it possible to diversify supramolecular architectures and physicochemical properties of systems.[1]

The interactions of cations with aromatic rings play an important role in a range of biological processes, including ion channels, membrane receptors and enzyme-supstrate interactions.[11] Amphiphilic molecules based on nucleosides, nucleotides and oligonucleotides attract significant attention due to their involvement in biochemical processes and their structural characteristics *i.e.* highly interactive polar head with additional hydrogen bonding and π-stacking capabilities.[1] Such compounds are finding more and more potentional role in biotechnological and biomedical applications,[12] as well as in applications such as catalysis, energy storage or transport of material.[13] Due to their affinity to bind different kinds of molecules, amphiphiles and other compounds containing pyridinium units are nowdays very actively examined in terms of novel, potential usage. For example, they bind with crown ethers[14,15], and calixarenes[16] in order to make novel functionalized, selective cages, and can

act as counter cations in complexes with some molecules making luminescent materials.[17] Moreover, such compounds are used as scaffolds for attaching various lipophilic compounds including fatty acids, and in that form are used for structure-activity correlations,[18] and nonviral gene delivery.[19] Making pyridinium based ionic liquids[20,21] is also of great interest, because they are environmentally benign solvents, have tunable polarity, coordinating ability, miscibilty in various liquids,[20] high thermal stability, low flammability, reusability and selectivity in chemical reactions.[21] Pyridinium based molecules also make polyelectrolyte gel-surfactant complexes in forms of stretched networks,[22] bind with three dimensional coordination polymers and anionic planar substances such as dyes,[17,23] naphthalene or benzenesulfonates.[23] Besides this, they are also used for making novel surfactants,[24–29] very often in their catanionic form that could be used in various applications mentioned previously. Such ion-pair amphiphiles are formed as the result of electrostatic interactions between oppositely charged headgroups, and they contain parent cationic and anionic surfactants in equimolar ratio, without inorganic counterions. Some pyridinium based compounds have already been characterized in terms of their thermal and thermotropic properties. Polymorphism and mesomorphism was obtained for the *N*-(*n*-alkyl) pyridinium hydrogensulfates.[24] Bis(*N*-alkyl pyridinium) tetrachlorocuprates exhibited hexagonal columnar, cubic[30] and smectic phases.[30,31] Hexadecylpyridinium 4-octylsulphate and 4-octylbenzenesulfonate and have shown rich thermal behavior, going through soft crystal formation and formation of smectic A and smectic B phases before isotropisation.[29]

Due to these interesting properties and their valuable usage, we have chosen pyridinium in the form of cationic surfactant, *i.e.* dodecylpyridinium chloride, to interact with three different compounds in their anionic form and as a result, to produce novel solid catanionic compounds. Biologically active anionic surfactant sodium cholate, synthetic anionic surfactant sodium dodecylbenzenesulfonate, and potassium picrate, compound that forms stable charge transfer complexes have been used for this purpose. Combination of techniques; microscopy, differential scanning calorimetry and powder X-ray diffraction, was used in order to obtain the effect of anionic constituent on structure and thermal behavior of synthesized compounds.

2. Experimental

2.1.Materials

Cationic surfactant dodecylpyridinium chloride (DPyCl, $C_{17}H_{30}NCl$, M_w = 283.89, Merck, Germany) and anionic surfactants, sodium cholate hydrate, *i.e.* 3a,7a,12a-trihydroxy-5b-cholanic-acid sodium salt (NaCh, $C_{24}H_{39}O_5Na$, Mw = 430.60; Sigma Ultra, min. 99%, Sigma Aldrich), sodium dodecylbenzene sulfonate (NaDBS; $C_{12}H_{25}C_6H_4SO_3Na$, Mw = 348.48; TCI Europe) were used for the preparation of solid salts. Potassium picrate, *i.e.* potassium 2,4,6-trinitrophenolate (KP, $C_6H_2N_3O_7K$, Mw = 267.20) was prepared and purified according the procedure described earlier.[32,33]

2.2. Preparation of surfactant molecular complexes

Solid molecular complexes **1**-**3** were prepared from equimolar aqueous solutions of components by high temperature mixing with magnetic stirrer for 20 minutes on elevated temperature and equilibrated undisturbed at least one week. The water used was purified by passing it through a Milli-Q Plus system until its specific conductivity fell below 0.10 μS cm^{-1}. The precipitated compounds were filtrated and washed with cold water to remove potentially coprecipitated electrolyte, dried under the vacuum and and stored protected from moisture and light before use. Novel 1:1 compounds precipitated as yellow (dodecylpyridinium picrate) and white (dodecylpyridinium cholate) needles, or as white powder (dodecylpyridinium dodecylbenzenesulfonate). According to Scheme 1 the examined complexes are abbreviated as: dodecylpyridinium picrate (compound **1**); dodecylpyridinium dodecylbenzenesulfonate (**2**); and dodecylpyridinium cholate (**3**).

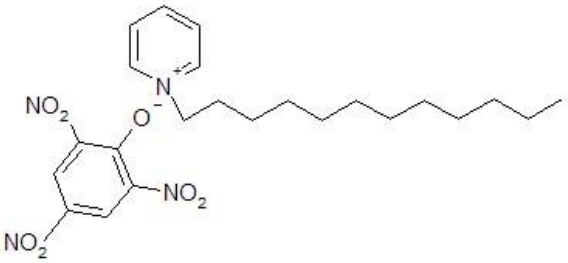

1

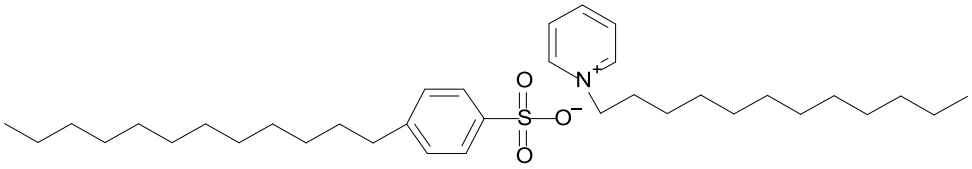

2

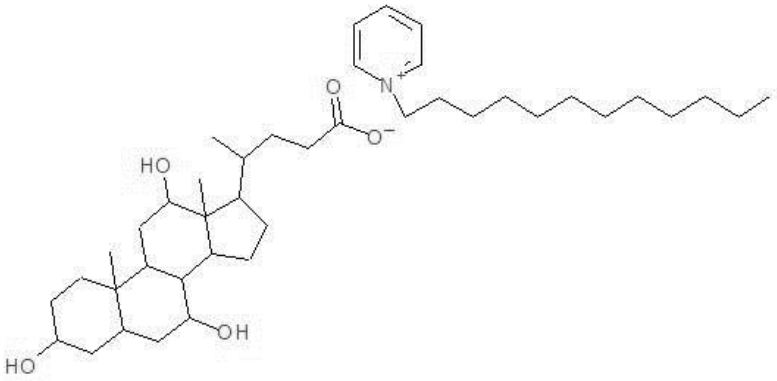

3

Scheme 1. The scheme of the examined catanionic compounds: dodecylpyridinium picrate (**1**); dodecylpyridinium dodecylbenzenesulfonate (**2**); dodecylpyridinium cholate (**3**).

2.3. Measurements

The identification of compounds was performed by elemental analysis (Perkin-Elmer Analyzer PE 2400 Series 2). Elemental analyses expressed as mass fraction in percent confirmed that the complexes were 1:1 (charge ratio) adducts and have high purity. Compound **1** $C_{23}H_{32}N_4O_7$, Mw = 476.53. Found: C, 57.94; H, 6.80; N, 11.77; requires C,

57.97; H, 6.78; N, 11.78 %. Compound **2**, $C_{55}H_{107}NO_3S$, Mw = 862.53. Found: C, 76.63; H, 12.54; N, 1.64; requires C, 76.59; H, 12.50; N, 1.62 %. Compound **3**, $C_{41}H_{69}NO_5$, M = 656.01. Found: C, 75.05; H, 10.60; N, 2.15; requires C, 75.06; H, 10.62; N, 2.14 %. Compound **3** was also analyzed spectroscopically, by NMR analysis (nuclear magnetic resonance spectroscopy; NMR Avance 600 Bruker with supraconducting magnet, 14 T field strength, frequency range 24-600 MHz and temperature range 223-373 K) according to the following designation:

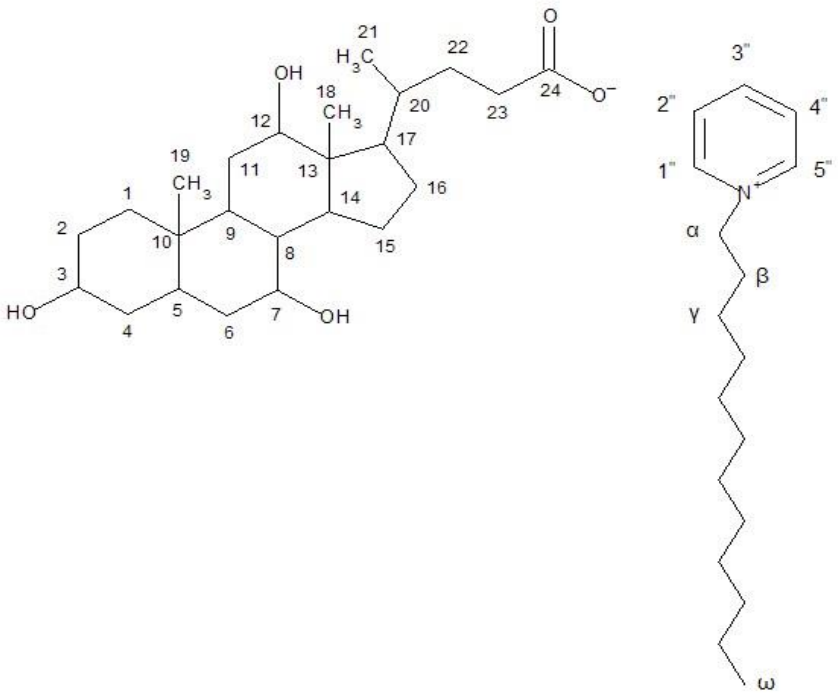

^{13}C NMR (150 MHz, DMSO-d_6) σ/ppm: 177.99 (C24), 145.42 (CHN_{py} (C2', C6')), 144.91 ($CCHC_{py}$ (C4')), 128.07 ($CCHC_{py}$ (C3', C5')), 71.13 (C12), 70.41(C3), 66.27 (C7), 60.62 (α-$CH_{2\ dodecyl}$), 46.49 (C17), 45.72 (C13), 41.58 (C5), 41.30 (C14), 39.56 (C8), 35.67 (C20), 35.54 (C1), 35.35 (C23), 34.89 (C10), 34.37 (C6), 32.80 (C22), 31.24 (β-$CH_{2\ dodecyl}$), 30.85 (γ-$CH_{2dodecyl}$), 30.35 (C2), 29.03- 28.69 ($(CH_2)_5$), 28.51 (C11), 28.46 (CH_2), 27.38 (C16), 26.18 (C9), 25.42 (CH_2), 22.86 (C15), 22.56 (C19), 22.07 (CH_2), 17.29 (C21), 13.89 (ω- CH_3), 12.38 (C18).

^{1}H NMR (600 MHz, DMSO-d_6) σ/ppm; 9.19 (2H, d, *J* = 5.8, CHN_{py} (C2', C6')), 8.61 (1H, t, *J* = 7.75, $CCHC_{py}$ (C4')), 8.16 (2H, t, *J* = 7.00, $CCHC_{py}$ (C3', C5')), 4.62 (2H, t, *J* = 7.4, α-$CH_{2\ dodecyl}$), 4.36 (1H, s br, OH (C3)), 4.09 (1H, s br, OH (C12)), 4.02 (1H, s br, OH (C7)), 3.78 (1H, s, CH (C12)), 3.60 (1H, s, CH (C7)), 3.20- 3.14 (1H, m, CH (C3)), 2.25-2.19 (1H, q, *J* =12.72, CH_2 (C4)), 2.19- 2.11 (1H, dt, *J* = 4.5, 4.9, CH (C9)), 1.99- 1.93 (1H, dt, *J*

=7.6, 4.63, CH (C14)), 1.93- 1.86 (3H, m, CH_2 (C23), CH_2 (C6), CH (C17)), 1.80- 1.67 (4H, m, CH_2 (C23), CH_2 (C16), β-$CH_{2\ dodecyl}$), 1.66- 1.58 (3H, m, CH_2 (C1), CH_2 (C15), CH_2 (C22)), 1.47-1.39 (4H, m, CH_2 (C4), CH_2 (C2), CH_2 (C11)), 1.38- 1.13 (24H, m, CH_2 (C6), CH (C8), CH_2 (C2), γ-CH_2, $(CH_2)_{8\ dodecyl}$, CH (C20), CH (C5), CH_2 (C16)), 1.12-1.04 (1H, m, CH_2 (C22)), 0.97- 0.89 (1H, m, CH_2 (C15)), 0.88 (3H, d, J = 6.5, CH_3 (C21)), 0.84 (3H, t, J = 6.9, ω-$CH_{3\ dodecyl}$), 0.82 (1H, m, partly under ω-$CH_{3\ dodecyl}$ peak, CH_2 (C1)), 0.80 (3H, s, CH_3 (C19)), 0.57 (3H, s, CH_3 (C18)).

Thermal behavior of synthesized compounds, as well as of their cationic component, dodecylpyridinium chloride, **DPyCl** was examined by the combination of different techniques: thermogravimetry, differential scanning calorimetry, microscopy and powder X-ray diffraction. Loss of the weight due to the heating (TG, *thermogravimetry*) was measured with the use of a Shimatzu DTG-60H. Samples were heated from room temperature to 573 K at the heating rate of 10 K min^{-1} in synthetic air flow of 50 mL min^{-1}. The temperature range for thermal analysis of each sample was determined by examination of TG and DTA curves. *Differential scanning calorimetry, DSC,* was carried out with a Perkin Elmer Pyris Diamond DSC calorimeter in N_2 atmosphere equipped with a model Perkin Elmer 2P intra-cooler in N_2 atmosphere, at the rate of 5 K min^{-1}. Temperature and enthalpy calibrations were performed using high purity standard (*n*-decane and indium). The transition enthalpy, ΔH/kJ mol^{-1}, was determined from the peak area of the DSC thermogram; and the corresponding entropy changes, ΔS/J mol^{-1} K^{-1}, were calculated using the maximal transition temperature. All results were taken only from the first heating and cooling run as mean values of several independent measurements carried out on different samples of the same compound. *Textures* were examined with Leica DMLS polarized optical light microscope, equipped with a Mettler FP 82 hot stage and Sony digital color video camera (SSC-DC58AP). *Diffraction patterns* were obtained by an automatic wide-angle X-ray powder diffractometer, Philips PW 3710, with monochromatized Cu Kα radiation (λ/Å = 1.54056) and proportional counter. Patterns were recorded at room temperature, RT. The overall diffraction angle region was $2\theta/^{o}$ = 3.0 – 60. The interlayer spacing (d_{hkl}) was calculated according to the Bragg's law.

3. Results and discussion

The formation of solid dodecylpyridinium catanionic compounds, **$[N^+Py(CH_2)_{11}CH_3]A^-$** is based on electrostatic interactions between negatively charged phenolic (compound **1**), sulfonate (**2**) and carboxylic (**3**) oxygen and positively charged nitrogen from dodecylpyridinium headgroup. As it was previously confirmed with elemental analysis, novel compounds are 1:1 ion-pair complexes, where formed electrolyte is removed by washing out and filtering. This synthesis can be described as anion-exchange reaction according to equation 1 (A^- denotes picrate, dodecylbenzenesulfonate or cholate in anionic form):

$$[N^+Py(CH_2)_{11}CH_3]Cl^- + Na^+A^- \rightarrow [N^+Py(CH_2)_{11}CH_3]A^- + Na^+ + Cl^- \quad (1).$$

Table 1. DSC results of different dodecylpyridinium salts, shown as transition temperatures, *T*/K, enthalpy changes, Δ*H*/kJ mol^{-1}, and entropy changes, Δ*S*/J mol^{-1} K^{-1}.

Compound	Heating			Cooling		
	T/K	Δ*H*/kJ mol^{-1}	Δ*S*/J mol^{-1} K^{-1}	*T*/K	Δ*H*/kJ mol^{-1}	Δ*S*/J mol^{-1} K^{-1}
DPy-Cl	343.87 418.46	46.25 0.30	134.50 0.72	417.05 407.76	- 0.43 - 0.05	- 1.03 - 0.12
1	308.68	9.42	30.52	No detectable changes Temporal hysteresis- crystallization next day		
2	380.24 424.93	7.57 0.77	19.56 1.82	422.03 367.08	- 0.75 - 7.74	- 1.78 - 21.09
3	382.56	19.03	45.91	Decomposition above 393 K		

Thermal properties of novel compounds were examined with the combination of techniques. Table 1 shows the resulting phase transition parameters (temperatures and related enthalpy and entropy changes) detected with differential scanning calorimetry. The nature of transitions was studied by polarizing microscopy, and the structure of compounds, as well as their thermotropic behavior was confirmed with powder X-ray diffraction (PXRD). Generally, the exsistence of sharp reflections in the ratio of 1 : 1/2 : 1/3 : 1/4 ... on the diffractograms is the confirmation of smectic layers *i.e.* lamellar structures in the one-dimensional lattice,[34] while the ratio of 1 : $1/\sqrt{3}$: $1/\sqrt{4}$: $1/\sqrt{7}$: $1/\sqrt{9}$: $1/\sqrt{12}$ ...is characteristic for hexagonal mesophases.[35]

First, we have decided to research thermal properties of the main component dodecylpyridinium chloride, **DpyCl**, before any examination on novel catanionic compounds. The sample dodecylpyridinium chloride was heated from room temperature (RT) to 425 K and cooled back to RT. This yellow crystalline powder shows rich thermal behavior (Table 1). In the heating cycle it goes through the melting process at relatively low temperature (343 K). Before isotropisation that begins at the temperature of 418 K, the liquid crystalline mesophase is detected, in forms of focal conic fan textures (Figure 1a). Previously examined 1-methyl-4-dodecylpyridinium chloride,[36] which differs from **DpyCl** only in the methyl group stacked on the pyridinium ring, showed melting without any thermotropic behavior. Three types of mesophases, smectic A, B and E were identified in *N*-alkylpyridinium halides substituted with a 4-methoxybiphenoxy group, with the individual molecules laterally arranged head to tail, bringing the anion close to positively charged pyridinium rings.[37,38] The similar structures with interdigitated molecules and sandwiched anions between pyridinium rings were described for the smectic A phase of 4-methyl-*N*-alkylpyridinium halides[39] and *N*-methyl-4-alkylpyridinium iodides.[36] Unlike these results, dodecylpyridinium chloride shows quite different type of LC mesophase. The **DPyCl** has already been examined in terms of thermal and thermotropic behavior[31], but the identified smectic mesophase is not in accordance with the mesophase that we have detected and proved. The textures resemble smectic ones, but PXRD of the sample taken at 383 K (Table 2) confirmed that this is type of 2D-hexagonal liquid crystal (LC) with diffraction reflections in the ratio of 1 : $1/\sqrt{3}$: $1/\sqrt{4}$ and unit cell dimension of a = 3.3 nm. Furthermore, crystallization in terms of LC formation occurs during cooling to RT, seen through mosaic (Figure 1b) and colorfull fan (Figure 1c) textures, and again, as hexagonal liquid crystal.

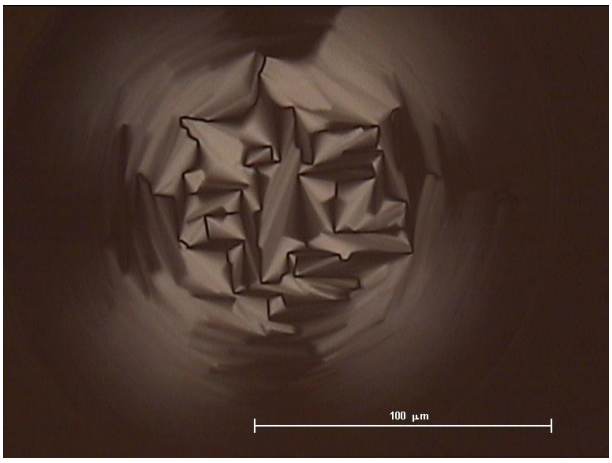

a

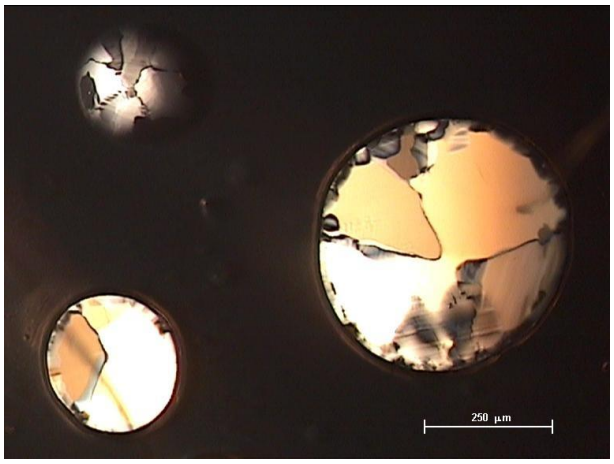

b

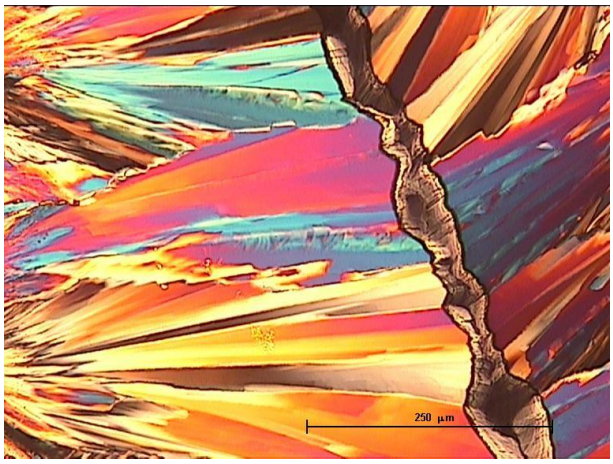

c

Figure 1. Micrographs of the solid **DPyCl**, observed during heating cycle, *T*/K = 360 (**a**) and slow cooling from the isotropic melt, *T*/K = 413 (**b**) and *T*/K = 298 (**c**). Scale bar represents 100 (**a**) 250 µm (**b**, **c**).

Table 2. Interplanar spacings, *d*, Miller indices, *hkl* or *hk* and relative intensities, I_{rel}, for dodecylpyridinium based compounds, obtained at different temperatures.

DPyCl, 383 K			**Compound 1, RT**			**Compound 2, 300 K**			**Compound 3, RT**		
d/Å	*hk*	I_{rel}	*d*/Å	*hkl*	I_{rel}	*d*/Å	*hkl*	I_{rel}	*d*/Å	*hkl*	I_{rel}
28.09	10	100	46.76	001	>100	27.22	001	100	24.80	001	>100
16.17	11	5	23.38	002	11.4	13.84	002	20	6.21	004	33
14.08	20	2	7.73	006	7.8	6.92	004	15	4.96	005	100
			6.73	007	17.9				4.15	006	30
			5.84	008	100	**Compound 2, 383 K**			3.12	008	11
			5.14	009	2.6	*d*/Å	*hkl*	I_{rel}	2.73	009	5
			4.66	0,0,10	17.9	25.52	001	100	2.09	0,0,12	6
			3.88	0,0,12	8.1	8.59	003	5	1.99	0,0,13	51
			3.61	0,0,13	7.1	4.70	006	1	1.79	0,0,14	2
			3.34	0,0,14	28.1						
			3.13	0,0,15	5.1						
			2.92	0,0,16	71.3						
			2.59	0,0,18	37.3						
			2.47	0,0,19	1.3						
			2.33	0,0,20	10.2						
			2.12	0,0,22	7.2						
			1.94	0,0,24	17.6						
			1.88	0,0,25	0.3						
			1.80	0,0,26	9.1						
			1.71	0,0,27	0.6						
			1.67	0,0,28	0.4						
			1.56	0,0,30	2.1						

Catanionic compounds containing dodecylpyridinium as the component behave completely different. Compound **1** *i.e.* the one that contains picrate as the anion, seemed crystalline at room temperature, but the PXRD of the sample displays sharp peaks with recognizable spacings in the ratio typical for smectic liquid crystals (Table 2, Figure 2). Obviously, compound **1** is in the form of crystal smectic with basic lamellar thickness of d_1 = 4.676 nm at room temperature having bilayer like structure (Table 2). Taking into calculations the length of dodecyl chain, l = 1.668 nm[40] and effective ionic radii of benzene part $å$ = 0.60 nm, and of trinitrophenolate $å$ = 0.70 nm,[40] the extended molecule has a length of d = 4.268 nm < 4.676 nm (Table 2, compound **1**). To conclude, the catanionic molecule is vertically arranged with fully extended dodecyl chain in this structure. There are no indications of the thermotropic mesomorphism, as was also found for previously examined picrates, for which analysis of crystallographic structures suggested that their solids are partly paraffin-like bilayers.[41] Moreover, similar arrangement was obtained for 3,5-dinitrobenzoic acid, 3,5-dinitrobenzamide and 3,5-dinitrobenzonitrile.[42] Two-dimensional planar sheets formed from their assemblies are stacked in a three-dimensional arrangement by π-π interactions, ranging from a simple stacking that resembles bilayer like structures, to a complex catenated networks.[42]

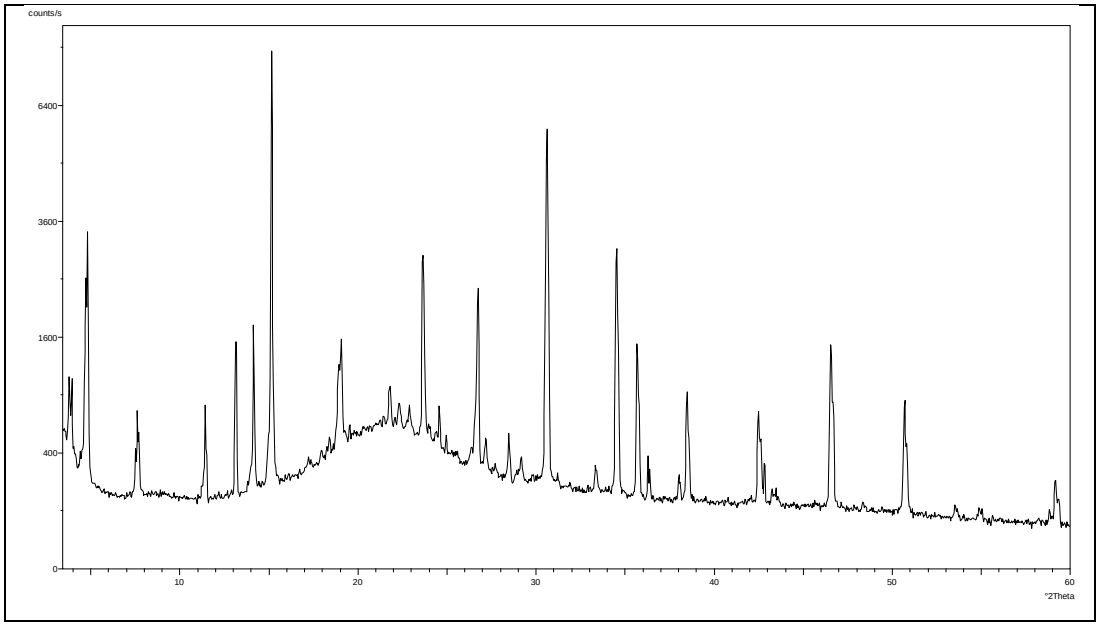

Figure 2. Diffractogram of the compound **1** taken at room temperature. Compound **1** is in the form of crystal smectic with basic lamellar thickness of d_1 = 4.676 nm.

Thermodynamic parameters of compound **1** (Table 1) point to relatively low transition temperature of melting at 308 K, with no corresponding exotherm in the cooling line, indicating a large temperature hysteresis, measurable in hours and associated to the presence of metastable states. Crystallization occurs the next day in forms of zig-zag blade textures (Figure 3a). It seems that these textures are typical for picrate complexes. They were also detected in the group of alkylammonium picrates with variable dodecyl chain number on the same amino headgroup[41] and picrate in combination with dodecylammonium cation.[43] The zig-zag blade crystalline textures of dodecyltrimethylammonium and didodeclydimethylammonium picrate developed 36 hours and of tridodecylmetylammonium picrate 54 hours after melting and cooling to room temperature, indicating again hysteresis.[41] From all these results, it is obvious that picrate anion promotes thermal properties of this compound. The absence of mesomorphic properties can be attributed to the dominant effect of picrate molecule, forming interlayer 3-D hydrogen bond network between pyridinium and picrate groups, where the ionic layer is "sandwiched" between the hydrocarbon chain layers. Since the Coulomb interactions in the ionic layer are stronger than van der Waals forces in the hydrocarbon layers, one would expect the unchanged ionic layers by heating, with conformational or positional disorder at lower temperatures. This disorder usually causes changes at higher temperatures, from the liquid crystalline phase to the isotropic liquid disorder. Unlike this, the existence of well-defined melting point, as only phase transition, indicates the disordering of dodecyl chains and the destruction of ionic layers simultaneously during melting. As the result, the liquid crystalline properties are not pronounced.[41]

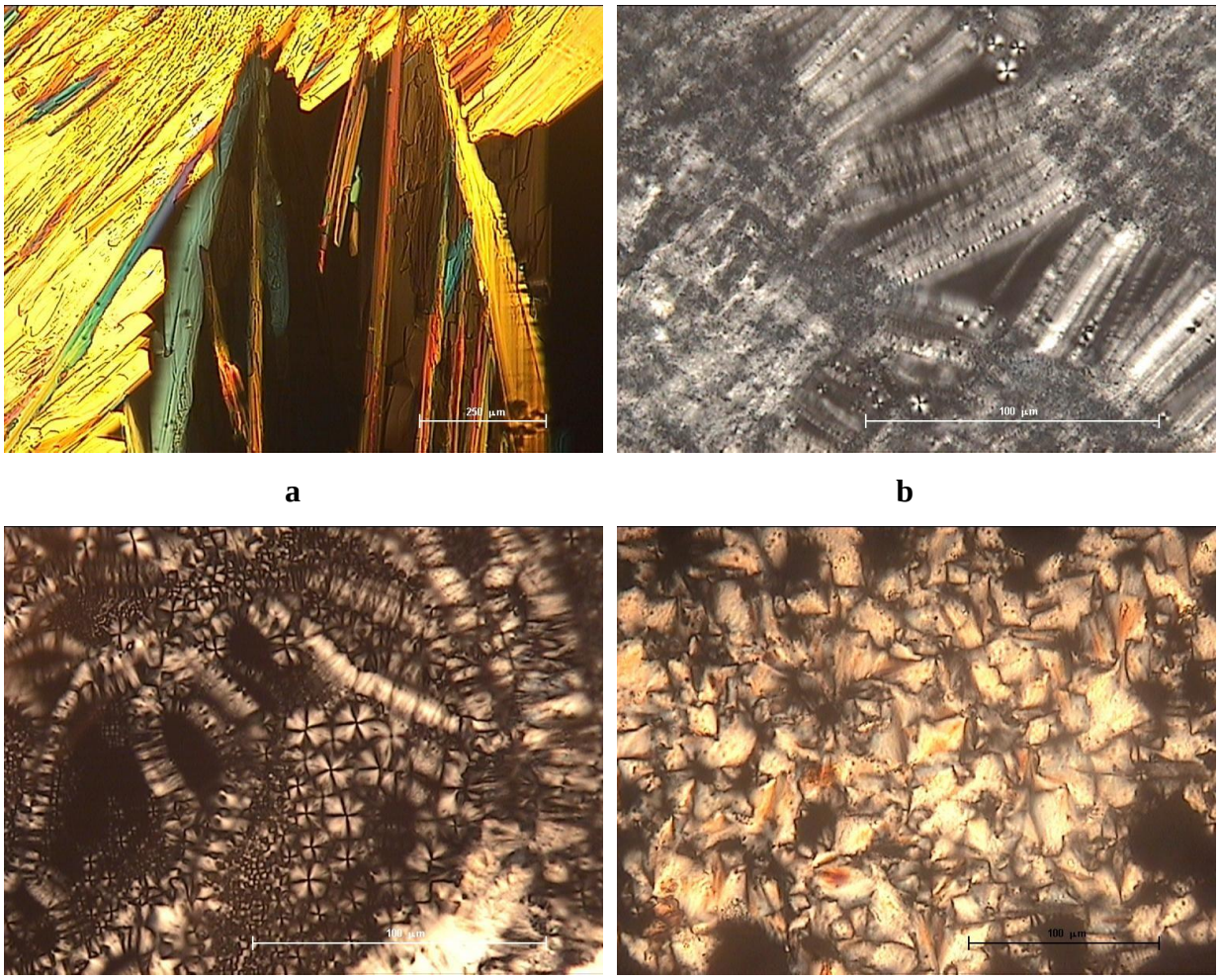

a **b**

c **d**

Figure 3. Textures of compound **1** (**a**) and compound **2** (**b**, **c** and **d**), observed at room temperature before heating (**b**) when heated, *T*/K = 390 K (**c**), cooled, *T*/K = 300 K (**d**), and the next day (**a**). Scale bar represents 100 (**b**, **c**, **d**) and 250 µm (**a**).

The transitions of catanionic dodecylpyridinium dodecylbenzenesulfonate, denoted as compound **2**, are classified as reversible. Compound **2** behaves very specific. First, the number of phase transitions is higher than for the samples **1** or **3**, indicating a more stepwise and complex processes.[29] Unlike compound **1**, the sample **2** shows thermotropic mesomorphism and is characterized as enantiotropic. Marques et al. previously obtained that the catanionics containing benzenesulfonate as the polar anion headgroup, showed distinct behavior when compared with the other compounds within their series.[29] Oily streaks of compound **2** (Figure 3b), can be seen at room temperature. Transition parameters given by DSC (Table 1) at 380 K may imply as smectic polymorphic transitions. Smooth focal-conic textures, and zip-like textures (Figure 3c) characteristic for smectic A phase are stable till

complete isotropisation at 424 K. Previously examined hexadecylpyridinium catanionic compounds, including hexadecylpyridinium 4-octylbenzenesulfonate, have also shown that the last phase observed prior to the isotropic liquid is the liquid crystalline smectic A phase.[29] Table 2 shows results of PXRD measurements that confirmed thermotropic mesomorphism and polymorphism of the sample **2**. Three sharp peaks with short range fluctuations and recognizable interlamellar distance and the ratio of spacings (1 : 1/2 : 1/4 at 300 K, 1 : 1/3 : 1/6 at 383 K) are displayed at both, 300 K and 383 K (Table 2). The breadth of the peaks and the fact that no higher angle peaks can be positively identified indicate that the sample is poorly ordered, but it can be identified as smectic LC, with lamellar thickness d_2 = 2.720 nm and at 300 K, and d_2 = 2.552 nm at 383 K. This is in accordance with benzenesulfonates properties; they are defined as amphiphilic molecules that cannot form well organized structures, cause microstructural changes, decrease membrane stability[44] and disrupt lamellar liquid-crystalline phase.[45,46] The crystallization of the sample **2** starts at 422 K on cooling, again in forms of smectic textures (Figure 3d), and LC-LC polymorphic transition. During heating and cooling scan the temperature interval of mesomorphic state, stretches in a whole temperature range of ~ 150 K. Having in mind the length of dodecyl chain, l = 1.668 nm[40,] effective ionic radii of benzene part $\mathring{a}$ = 0.60 nm, and of sulfonate group $\mathring{a}$ = 0.40 nm[40] the calculated length of extended catanionic molecule **2** is d = 6.536 nm. Therefore, the proposed arrangement in the bilayer at room temperature is fully extended catanionic molecule tilted at the angle of α = 24.20°. This is in accordance with the fact that in such type of poorly ordered phase, smectic A molecules are tilted at some angle (very similar as in the smectic C), giving smooth focal conic textures. As it was expected, the lamellar thickness changes by heating, indicating some structural changes, detected as polymorphism, whether molecules change their tilt angle, whether some major changes in the molecular arrangement occur, or maybe both of them simultaneously.

Table 2 also shows interplanar spacings, d, Miller indices, hkl, and relative intensities I_{rel}, of X-ray diffraction pattern for compound **3** taken at room temperature. The results of PXRD measurements made at room temperature refer to the smectic ordered phase, that is crystal smectic, with basic lamellar thickness of d_3 = 2.480 nm. The proposed arrangement is fully extended catanionic molecule of length d = 3.80 nm, tilted at the angle of α = 40.54°. The crystal smectic phase could be similar as was obtained in the bis(*N*-pentadecyl pyridinium) tetrachlorocuprate, with discrete cations and anions arranged in a lamellar fashion, alternation of hydrophilic and hydrophobic regions along one direction, with tilted

alkyl chains in the hydrophobic, and *N*-pentadecyl pyridinium acting as a promotor of extensive hydrogen bonding in the hydrophilic region.[30] When heated from room temperature, compound **3** exhibits melting 382 K, with partial degradation that ends with total decomposition and carbonization at 390 K.

The thermal phase behavior of the studied surfactants is highly dependent on the chemical nature of the polar headgroups. As it can be seen through the results of examined compounds, the anionic part of the molecule promotes the thermal behavior of the catanionic compound; the absence of mesomorphic properties and the formation of zig-zag blade textures in combination of dodecylpyridinium with picrate, thermotropic mesomorphism with polymorphism in terms of LC-LC transitions with dodecylbenzenesulfonate, and melting accompanied with degradation in combination with cholate. The affinity to form thermotropic mesophases, as well as their stability is dependent on the counter anions and the substitution pattern around the pyridinium core. Pyridine is chemically stable structure, providing a reactive nitrogen center, which is easily accessible for synthetic transformations into substituted mesogenic cation.[47] Different molecular conformations and associated conformational disorders are responsible for differences in the packing and the properties of the compounds in their solid state.[48] The driving forces for the formation of pyridinium mesogens are obviously hydrophobic interactions of the long alkyl substituents and ionic, dipole-dipole, cation-π interactions as well as π-π stacking of the aromatic cation core groups. Consequently, smectic liquid crystalline phases are often expected for pyridinium salts.[47] For example, in the stilbazolium based derivates of pyridinium, the presence of a donor methoxy group in 4'- position of the the aromatic system in the combination with the electron accepting pyridinium ring induces a large dipole moment in the molecule, and this leads to a stabilization of a liquid crystalline phase.[49]

It is well known that linear molecules favor LC formation more than branched ones.[50] Sample **2** has two linear dodecyl chains that promote the formation and stability of the mesophase.[51] Similar rich thermal behavior, *i.e.* polymorphism and mesomorphism was also obtained for the pyridinium compounds containing more than one linear alkyl chain, regardless of its length; *N*-(*n*-alkyl) pyridinium hydrogensulfates formed smectic B phases seen through fan shaped textures[24], bis(*N*-alkyl pyridinium) tetrachlorocuprates exhibited hexagonal columnar[31], cubic and smectic phases[31], and hexadecylpyridinium based catanionic surfactants have shown rich thermotropic behavior with formation of smectic A and smectic B phases.[29] However, for molecules **1** and **3** regardless of the *N*-alkyl group presence, the two

phenyl groups or hydrophobic steroid rings disable formation of liquid crystalline state.[51] The benzenesulfonate ion in compound **2** is structurally different from the other two anionic headgroups. The benzene ring has been found to be equivalent to 4-5 methylene groups on the alkyl chain.[52] The ring may also stabilize the sulfonate group by resonance, leading to charge density lowering, and hence being simultaneously part of the polar headgroup with delocalized charge, and also a part of the hydrophobic alkyl chain. This could lead to mutual stabilization of cationic and anionic polar headgroups, and in general stabilization of the whole molecule. The direct transition from solid state into isotropic liquid of sample **1**, and degradation of sample **3**, could be explained with the positive charge delocalized over the whole cationic aromatic pyridinium system thus weakening cation/anion electrostatic interactions between components.[50]

The geometric factors, *i.e.* the packing of the heads and chains, appear to be mainly reflected on their enthalpy and entropy values. The planar pyridinium cation is able to pack more closely with similar molecules, for example with picrate anion through π-π stacking, making more denser and ordered packing of compound **1**. Compound **3** containing the cholate anion shows higher transition enthalpy and entropy of melting than compound **1**, indicating higher disorder in the solid phase of the sample. The results point to a relatively complex interplay between geometric factors and electrostatic effects.[29]

The asymmetry of the hydrophobic parts is also one of the factors affecting the processes in thermal treatment. The comparison of catanionics shows that the thermal properties are closely correlated with the extent of symmetry in surfactant molecules. In general, the symmetrical catanionics, like compound **2**, with two dodecyl chains as the constituent parts of cationic and anionic surfactant, exhibit complex thermal behavior characterized by several successive phase transitions. Compounds often undergo reversible phase transitions in the cooling cycle, and in terms of mesophases are always enantiotropic. Temperatures of transitions as well as thermodynamic parameters change almost linearly with the total number of carbon atoms in hydrocarbon chains.[53] On the other hand, asymmetrical catanionics, like compounds **1** and **3**, have different number of phase transitions when compared heating and cooling cycles, with very often wide temperature hysteresis. Since the electrostatic interactions play a significant role in bilayers formed from both symmetrical and asymmetrical catanionics, the existence/difference between chain lengths of cationic and anionic part in catanionic molecule leads to a different and less ordered packing, and to more complex thermal behavior. The same chain length of both tails in a symmetrical catanionic

bilayer allows denser molecular packing than in a asymmetrical one.[53] As a consequence, the asymmetrical catanionics are often characterized as substances with disordered structure due to a poorer hydrophobic arrangement in the bilayer as well as total difficult arrangement of components into stable one.

4. Conclusions

Novel dodecylpyridinium based catanionic compounds were synthesized and characterized in terms of their thermal and potentional thermotropic behavior. The combination of techniques was used to examine their thermal properties; differential scanning calorimetry, powder X-ray diffraction, and optical polarizing microscopy. The thermal phase behavior of studied surfactants is highly dependent on the chemical nature of the anionic polar headgroup, its geometry, packing parameters and properties it possesses itself. The ability of the anionic constituent to promote these properties is seen through the diverse results of each of the examined catanionic compound. The asymmetry of the hydrophobic parts is also one of the factors affecting the processes in thermal treatment. Dodecylpyridinium picrate possesses crystal smectic properties at room temperature with the molecules vertically arranged and with fully extended dodecyl chains, making bilayer like structure. Crystallization in forms of zig-zag blade textures is temporally hindered. Like for dodecylpyridinium picrate, the results of PXRD measurements made on dodecylpyridinium cholate at room temperature refer also the crystal smectic phase, but with fully extended and tilted catanionic molecule. On the other hand, dodecylpyridinium dodecylbenzenesulfonate shows polymorphism and thermotropic mesomorphism, and is characterized as enantiotropic. Liquid crystalline phases were obtained in forms of oily streaks seen at room temperature, and smooth focal-conic and zip-like textures of SmA at higher temperature, with the fully extended and tilted catanionic molecules. The driving forces for the formation of pyridinium mesogens are obviously hydrophobic interactions of the long alkyl substituents and ionic, dipole-dipole, cation-π interactions as well as π-π stacking of the aromatic cation core groups.

Acknowledgments

The authors are pleased to acknowledge support of this work by the Ministry of the Science, Education, and Sport of the Republic of Croatia (Project No 098-0982915-2949). We are grateful to dr. sc. D. Matković-Čalogović, Faculty of Science, University of Zagreb, for X-ray diffraction measurements of the samples.

References

1. Zakharova, L.; Syakaev, V.; Voronin, M.; Semenov, V.; Valeeva, F.; Ibragimova, A.; Bilalov, A.; Giniyatullin, R.; Latypov, S.; Reznik, V.; Konovalov, A. *J. Colloid Interface Sci.* **2010**, *342*, 119–127.
2. Franke, D.; Egger, C. C.; Smarsly, B.; Faul, C. F. J.; Tiddy, G. J. T. *Langmuir* **2005**, *21*, 2704–2712.
3. Imai, M.; Yoshida, I.; Iwaki, T.; Nakaya, K. *J. Chem. Phys.* **2005**, *122*, 44906.
4. Singh, M.; Ford, C.; Agarwal, V.; Fritz, G.; Bose, A.; John, V. T.; McPherson, G. L. *Langmuir* **2004**, *20*, 9931–9937.
5. Oda, R.; Bourdieu, L.; Schmutz, M. *J. Phys. Chem. B* **1997**, 5913–5916.
6. Strey, R.; Schomäcker, R.; Roux, D.; Nallet, F.; Olsson, U. *J. Chem. Soc., Faraday Trans.* **1990**, *86*, 2253–2261.
7. Oda, R.; Huc, I.; Homo, J.-C.; Heinrich, B.; Schmutz, M.; Candau, S. *Langmuir* **1999**, *15*, 2384–2390.
8. Bergström, M.; Pedersen, J. S. *Langmuir* **1999**, *15*, 2250–2253.
9. Oda, R.; Huc, I.; Schmutz, M.; Candau, S. J.; MacKintosh, F. C. *Nature* **1999**, *399*, 566–569.
10. Liu, L.; Tan, G.; Agarwal, V.; Bose, A.; He, J.; McPherson, G. L.; John, V. T. *Chem. Commun.* **2005**, 4517–4519.
11. Hunter, C. A.; Low, C. M. R.; Rotger, C.; Vinter, J. G.; Zonta, C. *Proc. Natl. Acad. Sci. U S A* **2002**, *99*, 4873–4876.
12. Barthélemy, P. *Comptes. Rendus.Chimie* **2009**, *12*, 171–179.
13. Hainfeld, J. F. *PNAS* **1992**, *89*, 11064–11068.
14. Marchand, A. P.; Alihodžić, S.; McKim, A. S.; Kumar, K. A.; Mlinarić-Majerski, K.; Šumanovae, T.; Bott, S. G. *Tetrahedron Letters* **1998**, *39*, 1861–1864.
15. Moghimi, A.; Maddah, B.; Yari, A.; Shamsipur, M.; Boostani, M.; Fall Rastegar, M.; Ghaderi, A. R. *J. Mol. Struc* .**2005**, *752*, 68–77.
16. Ishihara, S.; Takeoka, S. *Tetrahedron Letters* **2006**, *47*, 181–184.
17. Binnemans, K.; Görller-Walrand, C. *Chem. Rev.* **2002**, *102*, 2303–2346.
18. Ilies, M. A.; Seitz, W. A.; Ghiviriga, I.; Johnson, B. H.; Miller, A.; Thompson, E. B.; Balaban, A. T. *J. Med. Chem.* **2004**, *47*, 3744–3754.

19. Bogatian, M. V.; Cimpeanu, C.; Deleanu, C.; Corbu, A. C.; Bogatian, G.; Balaban, T. S. *Commemorative Issue in Honor of Prof. Alexandru T. Balaban on the occasion of his 75th anniversary* **2005**, *2005*, 1–13.
20. Tourneux, E.; Gornitzka, H.; Marty, J.-D.; Lauth-de Viguerie, N. *Molecules* **2007**, *12*, 1940–1949.
21. Harjani, J. R.; Singer, R. D.; Garcia, M. T.; Scammells, P. J. *Green Chem.* **2008**, *10*, 436–438.
22. Sasaki, S.; Koga, S.; Sugiyama, M.; Annaka, M. *Phys. Rev. E. Stat. Nonlin. Soft Matter Phys.* **2003**, *68*, 021504.
23. Murakami, K. *Langmuir* **2004**, *20*, 8183–8191.
24. Stella, I.; Müller, A. *Colloids Surf. A* **1999**, *147*, 371–374.
25. Góralczyk, D.; Hąc, K.; Wydro, P. *Colloids Surf. A* **2003**, *220*, 55–60.
26. Pegiadou-Koemtzopoulou, S.; Papazoglou, V.; Kehayoglou, A. H. *J. Surfact. Deterg*. **2000**, *3*, 73–76.
27. Bakshi, M. S.; Kaur, I.; Sood, R. *Colloid. Polym. Sci.* **2003**, *281*, 928–934.
28. Kuiper, J. M.; Buwalda, R. T.; Hulst, R.; Engberts, J. B. F. N. *Langmuir* **2001**, *17*, 5216–5224.
29. Silva, B. F. B.; Marques, E. F. *J.Colloid Interface Sci.* **2005**, *290*, 267–274.
30. Francesco Neve, O. F. *Chem. Mater*. **2001**, *13* (6), 2032–2041
31. Taubert, A.; Steiner, P.; Mantion, A. *J. Phys. Chem. B* **2005**, *109*, 15542–15547.
32. Kudo, Y.; Wakasa, M.; Ito, T.; Usami, J.; Katsuta, S.; Takeda, Y. *Anal. Bioanal. Chem.* **2004**, *381*, 456–463.
33. Kudo, Y.; Usami, J.; Katsuta, S.; Takeda, Y. *Talanta* **2004**, *62*, 701–706.
34. Skoulios, A.; Luzzati, V. *Nature* **1959**, *183*, 1310–1312.
35. Luzzati, V.; Mustacchi, H.; Skoulios, A.; Husson, F. *Acta Cryst.* **1960**, *13*, 660–667.
36. Sudholter, E. J. R.; Engberts, J. B. F. N.; De Jeu, W. H. *J. Phys. Chem.* **1982**, *86*, 1908–1913.
37. Navarro-Rodriguez, D.; Frere, Y.; Gramain, P.; Guillon, D.; Skoulios, A. *Liq. Cryst.***1991**, *9*, 321–335.
38. Bravo-grimaldo, E.; Navarro-Rodríguez, D.; Skoulios, A.; Guillon, D. *Liq. Cryst.s* **1996**, *20*, 393–398.
39. Bazuin, C. G.; Guillon, D.; Skoulios, A.; Nicoud, J.-F. *Liq.Cryst.* **1986**, *1*, 181–188.
40. Lange, N. A.; Dean, J. A. *Lange's Handbook of chemistry*; McGraw-Hill, 1979.
41. Mihelj, T.; Štefanić, Z.; Tomašić, V. *J. Therm. Anal. Calorim.* **2012,** *108,* 1261-1272.

42. Arora, K. K.; PrakashaReddy, J.; Pedireddi, V. R. *Tetrahedron* **2005**, *61*, 10793–10800.
43. Tomašić, V.; Tušek-Božić, L.; Višnjevac, A.; Kojić-Prodić, B.; Filipović-Vinceković, N. *J. Colloid Interface Sci.* **2000**, *227*, 427–436.
44. Wieczorek, P. *J. Membr. Sci.* **1997**, *127*, 87–92.
45. Hodgdon, T. K.; Kaler, E. W. *Curr. Opin. Colloid Interface Sci.* **2007**, *12*, 121–128.
46. Guo, R.; Compo, M. E.; Friberg, S. E.; Morris, K. *J. Dispersion Sci. Technol.* **1996**, *17*, 493–507.
47. Binnemans, K. *Chem Rev.* **2005**, *105*, 4148–4204.
48. Gilson, D. F. R.; Kertes, A. S.; Manley, R. S. J.; Tsau, J.; Donnay, G. *Can. J. Chem.* **1976**, *54*, 765–8.
49. Guittard, F.; Taffin de Givenchy, E.; Geribaldi, S.; Cambon, A. *J. Fluorine Chem.* **1999**, *100*, 85–96.
50. Misaki, S.; Takamatsu, S.; Suefuji, M.; Mitote, T.; Matsumura, M. *Mol. Cryst. Liq. Cryst.* **1981**, *66*, 123–132.
51. Ster, D.; Baumeister, U.; Chao, J. L.; Tschierske, C.; Israel, G. *J. Mater. Chem.* **2007**, *17*, 3393–3400.
52. Blunk, D.; Praefcke, K.; Vill, V.; Demus, D.; Goodby, J.; Gray, G. W.; Spiess, H.-W.; Vill, V. In *Handbook of Liquid Crystals Set*; Wiley-VCH Verlag GmbH, 2008; pp. 305–340.
53. Filipović-Vinceković, N.; TomaŠić, V. In *Thermal Behavior of Dispersed Systems*; Garti, N., Ed.; M. Dekker Inc.: New York-Basel, 2000; Vol. 93, pp. 451–476.